Molecular Crystals and Liquid Crystals Science and Technology. Section A. Molecular Crystals and Liquid Crystals

Publication details, including instructions for authors and subscription information:
http://www.tandfonline.com/loi/gmcl19

Brillouin Scattering Study on o-Terphenyl Single Crystal

Shingo Kondo [a], Kenji Tamura [a] & Motosuke Naoki [a]

[a] Bioscience Department, Faculty of Engineering, Gunma University, Kiryu, Gunma, 376-8515, Japan

Version of record first published: 27 Oct 2006

To cite this article: Shingo Kondo, Kenji Tamura & Motosuke Naoki (2000): Brillouin Scattering Study on o-Terphenyl Single Crystal, Molecular Crystals and Liquid Crystals Science and Technology. Section A. Molecular Crystals and Liquid Crystals, 338:1, 223-241

To link to this article: http://dx.doi.org/10.1080/10587250008024432

Mol. Cryst. Liq. Cryst., Vol. 338, pp. 223-241
Reprints available directly from the publisher
Photocopying permitted by license only

Brillouin Scattering Study on *o*-Terphenyl Single Crystal

SHINGO KONDO*, KENJI TAMURA and MOTOSUKE NAOKI

Bioscience Department, Faculty of Engineering, Gunma University, Kiryu, Gunma 376–8515, Japan

(Received May 05, 1999)

Elastic waves in the *o*-terphenyl single crystal belonging to the orthorhombic system were measured by the Brillouin light-scattering spectroscopy. Wave vectors of elastic waves were obtained from three principal values of dielectric tensor determined by a new simple method. All nine elastic constants representing elastic contribution to the free energy have been determined, which show intermediate anisotropy between benzene and linear polyphenyls. The anisotropy can reasonably be explained from the arrangement of the phenyl bonds and the inter-molecular interactions caused from the packing of molecules in the crystalline lattice. It has been found that pure transverse elastic waves would not be observed in this system by the Brillouin scattering.

Keywords: *o*-Terphenyl single crystal; Brillouin scattering; elastic modulus tensor; dielectric tensor; total polarization

1. INTRODUCTION

o-Terphenyl supercools and vitrifies near the room temperature, and has extensively been investigated as one of typical molecular liquids[1–4]. Further, since *o*-terphenyl crystallizes slowly[5,6], its large single crystals can be prepared.

The pressure-volume-temperature (*P-V-T*) relations of the liquid, the supercooled liquid, the crystal, and the glass were previously presented, and the bulk modulus and the internal pressure (the bulk intermolecular force) of each state were determined[7]. The excess entropies of the liquid and the glass were analyzed and the communal entropy of molecular liquids was revealed[8]. Since the bulk quantities obtained above, however, correspond to those averaged over

* Correspondence Author.

space, effects of anisotropy of individual molecules on intermolecular interactions and configurations and on molecular motions are left unknown.

The collective motions, which reflect the intermolecular interactions in condensed matters, can be observed by light scattering. The Brillouin light scattering offers information on the propagation of the thermally excited acoustic modes of motions, i.e., the elastic waves. The frequency Ω is available from the Brillouin shift and the wave vector $\mathbf{K}$ from the scattering vector $\mathbf{q}$[9,10]:

$$\Omega = |\omega_s - \omega_i|, \tag{1}$$

$$\mathbf{K} = \mathbf{q} = \mathbf{k}_i - \mathbf{k}_s, \tag{2}$$

where ω and $\mathbf{k}$ are the angular frequency and the wave vector, respectively, and subscripts i and s denote the incident light and the scattered light, respectively. If the anharmonicity can be neglected, the harmonic term of the elastic potential energy is available from a set of frequencies and wave vectors.

In this work, we have determined the elastic term of the free energy and all components of the elastic modulus tensor for the *o*-terphenyl single crystal and have discussed the inter- and intra-molecular interactions. A simple method to obtain the principal values of the dielectric tensor, which is required for the evaluation of the scattering vector in anisotropic media, has also been developed for bodies with nervous surfaces.

2. ANALYSIS

The elastic properties of crystals are represented by the elastic terms of the free energy, F. In the harmonic approximation, F of the orthorhombic system is expressed by[11]

$$\begin{aligned} F =& \frac{1}{2}\lambda_{xxxx}u_{xx}^2 + \frac{1}{2}\lambda_{yyyy}u_{yy}^2 + \frac{1}{2}\lambda_{zzzz}u_{zz}^2 \\ &+ \lambda_{xxyy}u_{xx}u_{yy} + \lambda_{yyzz}u_{yy}u_{zz} + \lambda_{zzxx}u_{zz}u_{xx} \\ &+ 2\lambda_{xyxy}u_{xy}^2 + 2\lambda_{yzyz}u_{yz}^2 + 2\lambda_{zxzx}u_{zx}^2, \end{aligned} \tag{3}$$

where λ_{jklm} is the elastic modulus tensor, which has nine nonzero components for the orthorhombic system, and u_{jk} is the strain tensor relating to the j- and k-th components of the displacement vector $\mathbf{u}$ and the coordinates x_j and x_k by

$$u_{jk} = \frac{1}{2}\left(\frac{\partial u_j}{\partial x_k} + \frac{\partial u_k}{\partial x_j}\right), \tag{4}$$

Determination of elastic modulus tensor

In the medium with the density ρ, there are thermal molecular motions obeying the equation of motions[11]

$$\rho\ddot{u}_j = \lambda_{jklm}\frac{\partial^2 u_m}{\partial x_k \partial x_l}, \tag{5}$$

which represents the elastic waves. In the case of the monochromatic plane wave, i.e., $\mathbf{u} = \mathbf{u}_0 e^{i(\mathbf{K}\cdot\mathbf{r}-\Omega t)}$, $\mathbf{u}$, Ω, and $\mathbf{K}$ satisfy the following equations:

$$(\rho\Omega^2\delta_{jm} - \lambda_{jklm}K_kK_l)u_m = 0, \tag{6}$$

$$|\rho\Omega^2\delta_{jm} - \lambda_{jklm}K_kK_l| = 0, \tag{7}$$

where δ_{jm} is Kronecker's delta. For some special wave vectors, eqs. (6) and (7) take simple form. For examples, these follow for $\mathbf{K}(K_x, 0, 0)$

$$\rho\Omega^2 = \lambda_{xxxx}K_x^2;\ u_x \neq 0,\ u_y = u_z = 0, \tag{8}$$

$$\rho\Omega^2 = \lambda_{xyxy}K_x^2;\ u_y \neq 0,\ u_x = u_z = 0, \tag{9}$$

$$\rho\Omega^2 = \lambda_{zxzx}K_x^2;\ u_z \neq 0,\ u_y = u_x = 0, \tag{10}$$

and for $\mathbf{K}(K_x, K_y, 0)$

$$\rho\Omega^2 = \lambda_{zxzx}K_x^2;\ \lambda_{yzyz}K_y^2;\ u_z \neq 0, u_y = u_x = 0, \tag{11}$$

$$\begin{aligned}(\rho\Omega^2)_\pm &= \frac{1}{2}[(\lambda_{xxxx}+\lambda_{xyxy})K_x^2 + (\lambda_{xyxy}+\lambda_{yyyy})K_y^2 \\ &\pm\sqrt{\{(\lambda_{xxxx}-\lambda_{xyxy})K_x^2+(\lambda_{xyxy}-\lambda_{yyyy})K_y^2\}^2+4\{(\lambda_{xxyy}+\lambda_{xyxy})K_xK_y\}^2}]; \\ \left(\frac{u_y}{u_x}\right)_\pm &= 1/\{2(\lambda_{xyxy}+\lambda_{xxyy})K_xK_y\}[(-\lambda_{xxxx}+\lambda_{xyxy})K_x^2+(-\lambda_{xyxy}+\lambda_{yyyy})K_y^2 \\ &\pm\sqrt{\{(\lambda_{xxxx}-\lambda_{xyxy})K_x^2+(\lambda_{xyxy}-\lambda_{yyyy})K_y^2\}^2+4\{(\lambda_{xxyy}+\lambda_{xyxy})K_xK_y\}^2}], \\ u_z &= 0.\end{aligned} \tag{12}$$

Similar expressions can be obtained for $\mathbf{K}(0, K_y, 0)$, $\mathbf{K}(0, 0, K_z)$, $\mathbf{K}(K_x, 0, K_z)$, and $\mathbf{K}(0, K_y, K_z)$. In the elastic waves ruled by the equations such as eqs. (8)-(11), the displacements are parallel or perpendicular to $\mathbf{K}$. We call these states as "pure-longitudinal" or "pure-transverse" denoted by 1_p or t_p. On the other hand, in the elastic waves ruled by the equations such as eq. (12), the displacements are neither parallel nor perpendicular to $\mathbf{K}$, i.e., $\mathbf{K}\cdot\mathbf{u} \neq 0$ and $\mathbf{K}\times\mathbf{u} \neq 0$. These waves are called as "pseudo-longitudinal" or "pseudo-transverse" wave denoted by 1_{mix} or t_{mix}.

The elastic modulus tensor can be determined from the frequencies of the elastic waves with adequate independent wave vectors. Since the wave vectors of the elastic waves are obtained from those of the light in the sample (see eq. (2)), the refractive index in the propagation direction of the light, i.e., the dielectric tensor, is necessary.

Determinations of refractive index and dielectric tensor

The *o*-terphenyl crystal belongs to the biaxial crystal, in which the propagation of the electromagnetic waves is usually complicate, except some certain directions and polarizations[9,12]. The wave vector **k**, the electric field **E**, and the energy flux vector (Poynting vector) **S** of the electromagnetic wave in the biaxial crystal can be obtained from the following equations.

$$\mathbf{k} = \omega_0/c_0\mathbf{n}, \tag{13}$$

$$\mathbf{S} = [\mathbf{E} \times \mathbf{H}] = \varepsilon_0 c_0 \{\mathbf{n}E^2 - \mathbf{E}(\mathbf{E} \cdot \mathbf{n})\}, \tag{14}$$

$$(n^2\delta_{jk} - n_j n_k - \varepsilon_{jk})E_k = 0, \tag{15}$$

$$|n^2\delta_{jk} - n_j n_k - \varepsilon_{jk}| = 0, \tag{16}$$

where ω_0 is the frequency of light, c_0 is the velocity of light in vacuum, and ε_0 and ε_{jk} are the vacuum permittivity and the dielectric tensor, respectively. The magnitude of **n** gives the refractive index along its direction.

Here and what follows, we use the coordinates coincident with the principal dielectric axes. In the case that the light propagates in the *xy*-plane, i.e., $n_z = 0$, the following expressions can be obtained,

$$n^2 = \varepsilon^{(z)}; \quad E_z \neq 0, \quad E_x = E_y = 0, \tag{17}$$

$$\frac{n_x^2}{\varepsilon^{(y)}} + \frac{n_y^2}{\varepsilon^{(x)}} = 1; \quad \frac{E_x}{E_y} = -\frac{\varepsilon^{(y)} n_y}{\varepsilon^{(x)} n_x}, \quad E_z = 0, \tag{18}$$

where $\varepsilon^{(x)}$, $\varepsilon^{(y)}$, and $\varepsilon^{(z)}$ are the principal values of the dielectric tensor.

When the light is polarized perpendicular to the coordinate *xy*-plane, i.e., parallel to *z* axis, eqs. (13), (14), and (17) lead that the refractive index $n_\perp$ is independent of the direction and that the direction of **S** coincides with that of **k**. Therefore, the ordinal law of the refraction holds on a boundary plane (a crystal face) parallel to *z* axis:

$$\frac{n_\perp}{n_a} = \frac{\sin\theta_i}{\sin\theta_r}; \quad n_\perp = \sqrt{\varepsilon^{(z)}}, \tag{19}$$

where θ_i and θ_r are the angle of incidence and refraction, respectively, and n_a is the refractive index of the surrounding medium. The light polarized perpendicular to the incident plane is called as "in the s-state" and that polarized parallel to the incident plane is called as "in the p-state".

When the light is polarized parallel to the coordinate *xy*-plane, eqs. (14) and (18) lead to

$$\frac{S_y}{S_x} = \frac{\varepsilon^{(y)} n_y}{\varepsilon^{(x)} n_x}. \tag{20}$$

Eqs. (18) and (20) indicate that the direction of **k** differs generally from that of **S** and that the refractive index $n_{\|}$ depends on the direction of **k**, i.e., **n**. For the light incident upon a boundary plane (a crystal face) parallel to z axis in the p-state, its directional angle of the wave vector from x axis becomes $\alpha + \pi - \theta_n$ in the crystal and

$$\frac{n_y}{n_x} = \tan(\alpha + \pi - \theta_n), \tag{21}$$

$$\frac{n_{\|}}{n_a} = \frac{\sin\theta_0}{\sin\theta_a}, \tag{22}$$

$$n_{\|}{}^2 = n_x^2 + n_y^2, \tag{23}$$

where α is the angle of the outer normal of the crystal face from x axis, θ_0 is the incident angle being positive in a clockwise direction, and θ_n is the angle of refraction. From eqs. (18) and (21) – (23), $n_{\|}$ for the p-state is expressed in terms of θ_0 as

$$(n_{\|}^2 - \varepsilon^{(x)}) = \left(1 - \frac{\varepsilon^{(x)}}{\varepsilon^{(y)}}\right)(\cos\alpha\sqrt{n_{\|}^2 - n_a^2\sin^2\theta_0} + n_a\sin\theta_0\sin\alpha)^2. \tag{24}$$

One way of the estimation of $\varepsilon^{(x)}$, $\varepsilon^{(y)}$, and $\varepsilon^{(z)}$ is to measure the angle of the total polarization θ_p. The energy flux of the light polarized parallel to the incident plane (the p-state) is not reflected at the incident angle of θ_p on a boundary plane having the incident plane coincident with the coordinate plane. Relations among θ_p, the angle of refraction θ_n, the refractive index n_p, and the angle of refraction θ_s for the energy flux vector **S** can be written (see Appendix) as

$$\sin\theta_p\cos\theta_p\left(\frac{1}{\tan\theta_n} + \tan\theta_s\right) = 1, \tag{25}$$

$$\frac{\sin\theta_p}{\sin\theta_n} = \frac{n_{\|}}{n_a} = n_p, \tag{26}$$

$$\tan(\alpha - \theta_s) = \frac{\varepsilon^{(y)}}{\varepsilon^{(x)}}\tan(\alpha - \theta_n). \tag{27}$$

Eliminating θ_n and θ_s from eqs. (25) ~ (27), we have the equation for the refractive index n_p as

$$PX^2 - QX + R = 0, \tag{28}$$
$$P = \cos\theta_p(\gamma\tan^2\alpha + 1),$$
$$Q = 2(\gamma - 1)\sin\theta_p\cos\theta_p\tan\alpha + \gamma\tan^2\alpha + 1,$$
$$R = \sin\theta_p\{\sin\theta_p\cos\theta_p(\tan^2\alpha + \gamma) + (\gamma - 1)\tan\alpha\},$$

where

$$X = \sqrt{n_p^2 - \sin^2 \theta_p}, \tag{29}$$

$$\gamma = \frac{\varepsilon^{(y)}}{\varepsilon^{(x)}}. \tag{30}$$

Since $\varepsilon^{(y)}$ is expressed from eqs. (18), (21), (23), (26), (29), and (30) as

$$\varepsilon^{(y)} = \frac{n_a^2 n_p^2 \{(X + \sin\theta_p \tan\alpha)^2 + \gamma(X \tan\alpha - \sin\theta_p)^2\}}{(\tan^2\alpha + 1)(X^2 + \sin^2\theta_p)}, \tag{31}$$

values of $\varepsilon^{(x)}$ and $\varepsilon^{(y)}$ can be obtained by adjusting γ so as to have the same values of $\varepsilon^{(y)}$ for θ_p measured on (more than two) independent crystal faces that are perpendicular to the xy plane. $\varepsilon^{(z)}$ can be obtained from θ_p measured in the another coordinate planes.

If $\varepsilon^{(x)} = \varepsilon^{(y)}$, eqs. (25) ~ (27) reduce to

$$\tan\theta_p = n_p, \tag{32}$$

$$n_p = 1. \tag{33}$$

The former is the Brewster's law and the latter represent that the refractive indexes of both media are the same.

3. EXPERIMENTAL

Material

o-Terphenyl sample purchased from Tokyo Chemical Ind. Co. was purified by repeated recrystallizations from methanol solution. Three transparent single crystals with sufficient dimensions (ca. 7 × 7 × 30 mm) for optical measurements were prepared for the Brillouin light scattering. The form of the *o*-terphenyl single crystals is essentially the same as that in literature[5]. Relations among the crystallographic axes, the Cartesian coordinates, and the principal dielectric axes used in the present work are illustrated in Figure 1. The crystallographic and thermodynamic data are listed in Table I[7,13].

Brillouin light scattering

A schematic diagram of the Brillouin light-scattering spectrometer is shown in Figure 2. The monochromatic light with the wave length of 488 nm generated by an Ar-ion laser equipped with an air-space etalon was focalized in the sample

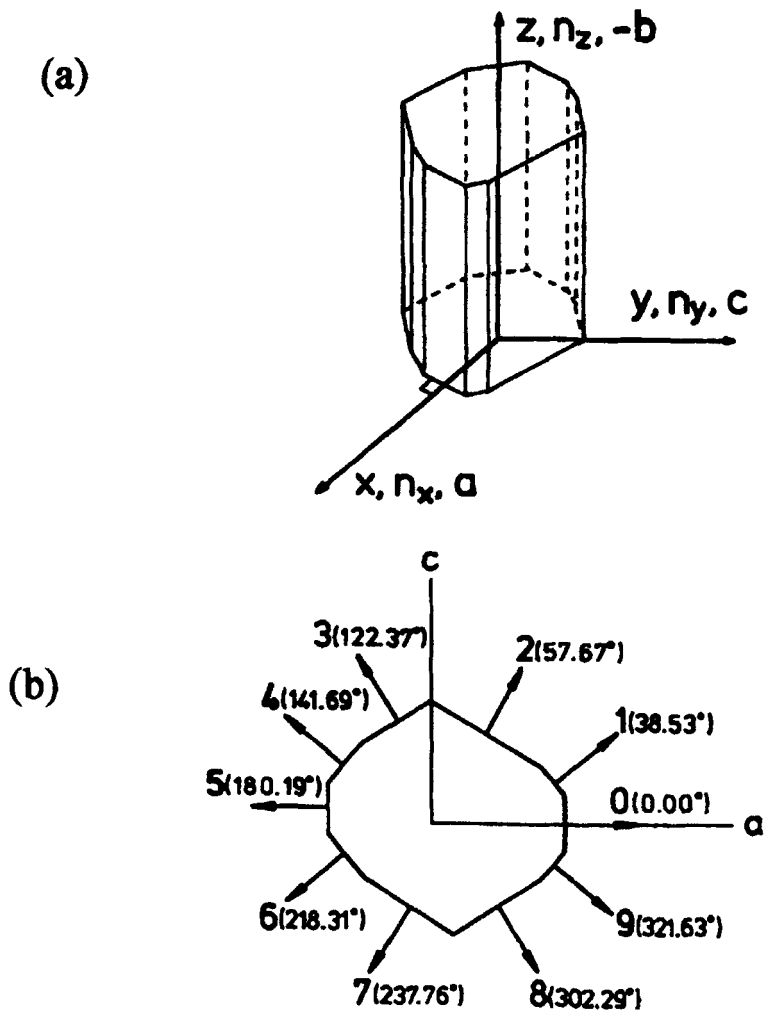

FIGURE 1 a) The form of *o*-tephenyl single crystals. (x, y, z): elasticity, (n_x, n_y, n_z): optics, and (a, b, c): crystallography. b) Crystal faces, their normal vector, and facial angles measured from a axis

through a lens with the focus length of 0.6 m after adjusting its polarization with a half wave plate and a Glan-Thomson prism. The light scattered in the angle $\theta \pm 1°$ with a polarization aimed at was collimated through a lens with the focus length of 0. 1 m and was analyzed with a Burleigh RC-110 five-pass Fabry-Perot interferometer operated at an optimum free spectral range. The output of the interferometer was transmitted into a photon-counting system assembled with a

Hamamatsu R464 photomultiplier tube and a NAIG E multichannel scalar system. The Brillouin spectrum was accumulated over 2000 sweeps of the interferometer and was traced with a Hewlett Packard 7004B X-Y recorder over two free spectral ranges. The instrumental finess estimated from the line width of unshifted component (the Rayleigh line) was about 60. The temperature of the sample was controlled to 25 ± 0.5 °C.

TABLE I Characteristics of the *o*-terphenyl crystal at 25 °C

Crystal system[a]		*orthorhombic* ($P2_12_12_1$)
Axial lengths[a],	a / nm	1.86
	b / nm	0.605
	c / nm	1.18
Number of molecules in unit cell[a]		4
Density[b],	ρ / kg m^{-3}	1165.22 ± 0.30
Thermal expansion coefficient[b],	$\alpha \times 10^4$ / K^{-1}	2.470 ± 0.0017
Heat capacity at constant P[c],	C_P / J K^{-1}mol^{-1}	276.6
Heat capacity at constant V[c],	C_V / J K^{-1}mol^{-1}	261.9
Isothermal bulk modulus[b],	κ_T / GPa	4.078 ± 0.005
Adiabatic bulk modulus[b],	κ_S / GPa	4.308 ± 0.005

a. Clews and Lonsdale (Ref. [5]).
b. Naoki and Koeda (Ref. [7]).
c. Chang and Bestul (Ref [13]).

According to the wave vectors required (Figure 3), three types of the setting of the crystal were used. The peak frequency ν_B, the line width at half height Δ_B, and the integrated intensity I_B of each shifted doublet (the Brillouin lines) were measured together with the line width Δ_c of the central component (the Rayleigh line). Assuming Δ_c to be equal to the instrumental width, the true Brillouin line width Δ was obtained from Δ_B by subtraction of Δ_c.

Principal values of the dielectric tensor

The principal axes are sought as those when the field of a cross-Nicol became dark. θ_p for the blue light was measured for each crystal faces in both clockwise and counter clockwise directions. $\varepsilon^{(x)}$ and $\varepsilon^{(y)}$, were so determined as to minimize the deviation of $\varepsilon^{(x)}$ calculated from θ_p with eqs. (30) and (31). $\varepsilon^{(z)}$ was estimated from $\varepsilon^{(x)}$ and θ_p measured for a crystal face having the incident plane coincide with the zx-plane (Figure 1).

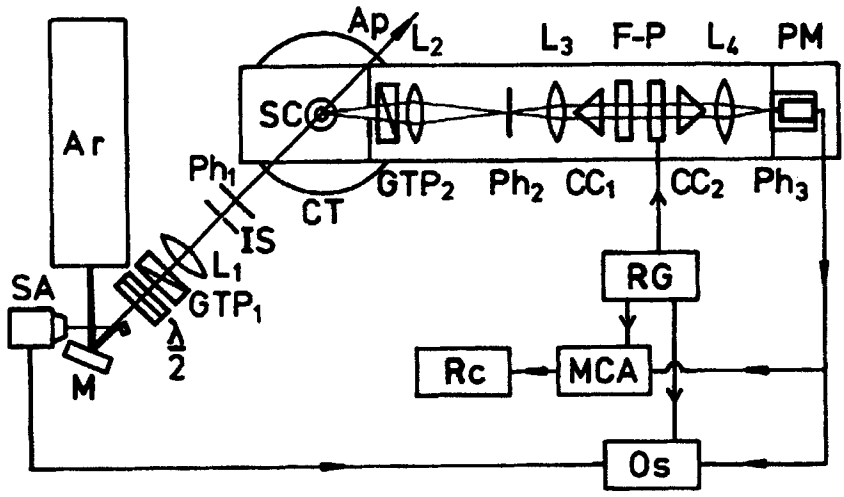

FIGURE 2 A scheme of the Rayleigh-Brillouin light scattering spectrometer. Ar: Ar-ion laser, SA: spectrum analyzer, M: mirror, λ/2: half wave plate, GTP: Glan-Thomson prism, L: lens, IS: iris stop, Ph: pinhole, CT: circular table, SC: sample cell, Ap: apeture, CC:corner cube, F-P: Fabry-Perot interferometer, PM: photomultiplier tube, RG: ramp generator, Os: oscilloscope, MCA: multichannel analyzer, and Rc: recorder

4. RESULTS

The *o*-terphenyl single crystal showed one distinct zone axis, which corresponded with one of the principal dielectric axes. Another principal dielectric axis was found to be perpendicular to a pair of parallel crystal faces. These axes have been found to be coincide with the crystallographic axes. Any face perpendicular to the other principal dielectric axis was not found. As a matter of convenience, we will take Cartesian coordinated in which *x*, *y*, and *z* axes correspond to *a*, *c*, and *b* crystallographic axes, respectively (Figure la). The facial angles measured from *x* axis are shown in Figure 1b. The principal values of the dielectric tensor estimated from θ_p are listed in Table II. The experimental errors in $\varepsilon^{(x)}$and $\varepsilon^{(y)}$ are about 0.7 % and the errors in $\varepsilon^{(z)}$ may be somewhat larger than those. The fairly large uncertainty $\varepsilon^{(x)}$ may come from the difficulty in determination of θ_p and from a lack of the flatness of the crystal faces.

TABLE II The principal values of the dielectric tensor for blue light (488 nm)

$\varepsilon^{(x)}(=\varepsilon^{(a)})$	2.972 ± 0.021
$\varepsilon^{(y)}(=\varepsilon^{(c)})$	2.627 ± 0.019
$\varepsilon^{(z)}(=\varepsilon^{(b)})$	2.879

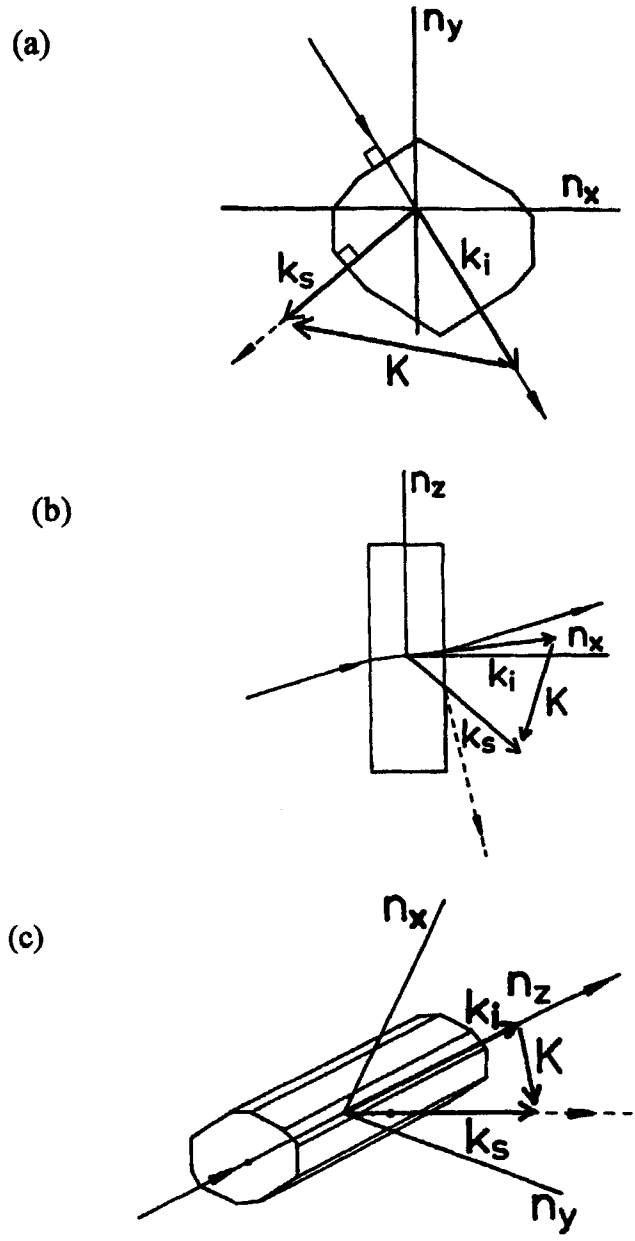

FIGURE 3 Three types of the scattering geometry. a) $\mathbf{K}(K_x, K_y, 0)$, b) $\mathbf{K}(K_x, 0, K_z)$, and c) $\mathbf{K}(K_x, K_y, K_z)$

One or two Brillouin doublets were observed in all VV spectra and in some HH spectra, but no Brillouin spectrum could be detected in the VH and HV spectra, except the wave vectors of $\mathbf{K}(K_x, K_y, K_z)$. Two examples of the spectra are shown in Figure 4. Frequencies and wave vectors of the Brillouin lines are listed in Table III. Deviations in the Brillouin frequency are within ±1 % among three *o*-terphenyl single-crystal samples and among different pairs of crystal faces that offer the same wave vectors. Deviations in the attenuation coefficient $\alpha\lambda_s$ $(= \pi\Delta/\nu_B)$ per one wave length are considerably large (0.04 – 0.07) among the samples and the pairs of the crystal faces.

TABLE III The wave vectors and frequencies of the observed elastic waves together with the frequencies calculated from the elastic constants and directional angles of the wave vectors and displacement vectors from *x* axis

Wave vector in 10^7 m^{-1}			*Frequency in GHz*		*Angle in degre*		
Kx	*Ky*	*Kz*	*observed*	*calculated*	***K***	***u***	
2.34	0	0	12.46	12.46	0	0	l_p, 13.09 GPa
3.35	1.83	0	19.61	19.66	29	23	l_{mix}
			9.65	9.54		113	t_{mix}
0.55	0.49	0	3.62	3.62	42	34	l_{mix}
			1.77	1.79		124	t_{mix}
1.02	1.83	0	9.53	9.63	61	51	l_{mix}
			5.20	5.19		141	t_{mix}
0	3.70	0	15.47	15.47	90	90	l_p, 8.07 GPa
3.85	0	1.12	20.76	21.06	16	11	l_{mix}
2.09	0	2.09	13.85	13.96	45	32	l_{mix}
			6.64	6.69		122	t_{mix}
0.39	0	1.21	5.13	5.06	72	59	l_{mix}
			3.13	3.03		149	t_{mix}
0	0	1.82	6.76	6.76	90	90	l_p, 6.34 GPa
0	2.22	2.22	13.55	13.68	45	41	l_{mix}, from *y* axis
1.16	1.85	2.22	14.02	13.91			
			7.63	7.69			

As the directions of the dielectric principal axes of *o*-terphenyl coincide with those of the crystallographic axes, we have assumed the principal axes of the stress and strain tensors also coincide with the crystallographic axes. Then values of three components of the elastic tensor can be estimated as 13.09 GPa from $\mathbf{K}(K_x, 0, 0)$, 8.07 GPa from $\mathbf{K}(0, K_y, 0)$, and 6.34 GPa from $\mathbf{K}(0, 0, K_z)$, which

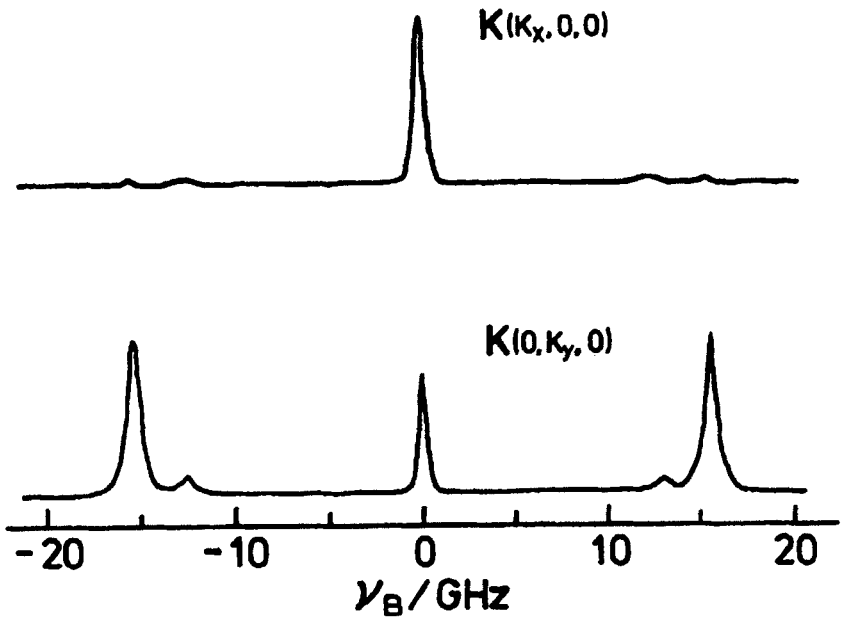

FIGURE 4 Examples of the Brillouin spectra (VV polarization). The crystal faces used for the incidence and observation are respectively No. 7 and No. 3 for $K_x = 2.34 \times 10^7$ m^{-1} and No. 8 and No. 7 for $K_y = 3.70 \times 10^7$ m^{-1}, which are shown in FIGURE 1b

are listed in Table III. The differences between the elastic modulus estimated from the VV spectra and those from the HH spectra are at most 6 %.

Since the longitudinal elastic waves can generally be observed in the VV and HH spectra[9], we have assumed that $\lambda_{xxxx} = 13.09$ GPa, $\lambda_{yyyy} = 8.07$ GPa, and $\lambda_{zzzz} = 6.34$ GPa. The another six components of the elastic modulus have been obtained by fitting procedures, i.e., λ_{xxyy} and λ_{xyxy} from eq (12) and $\rho\Omega^2$ with $\mathbf{K}(K_x, K_y, 0)$, λ_{zzxx} and λ_{zxzx} from a equation similar to eq (12) and $\rho\Omega^2$ with $\mathbf{K}(K_x, 0, K_z)$, λ_{yyzz} and λ_{yzyz} from eq (7) and $\rho\Omega^2$ with $\mathbf{K}(K_x, K_y, K_z)$. Values of the elastic moduli are listed in Table IV in crystallographic notations. The deviation in the frequency of the elastic wave from that calculated with the elastic modulus tensor is at most ± 3% as shown in Table III.

It has been found that all of the observed Brillouin spectra correspond to the pure or pseudo longitudinal elastic waves or the pseudo transverse elastic waves. The pure longitudinal waves are designated by 1_p in Table III. It is notable matter that no pure transverse elastic waves ruled by eq. (11) type equations could be observed by the Brillouin scattering.

TABLE IV Elastic constants of polyphenyls in GPa

	o-terphenyl	*benzene*[a]	*biphenyl* (D_{10})[b]	*p-terphenyl*[b]
c_{11}	13.09	6.14	7.58	8.18
c_{22}	6.34	6.56	9.01	9.75
c_{33}	8.07	5.83	18.06	26.42
c_{12}	4.23	3.52	~5	~5.5
c_{13}	4.75	4.01	3.95	4.33
c_{23}	1.39	3.90	7.75	~8. 1
c_{44}	4.63	1.97	2.13	3.36
c_{55}	3.08	3.78	2.20	2.70
c_{66}	2.94	1.53	4.59	5.13

a. Heseltine, Elliott, and Wilson (Ref. [14]).
b. Ecolivet and Sanquer (Ref. [15]). Components of c_{15}, c_{25}, c_{35}, and c_{46} are omitted.

5. DISCUSSION

The elastic moduli of *o*-terphenyl show larger anisotropy than benzene[14], but smaller than biphenyl and *p*-terphenyl[15], which are compared in Table IV. Ecolivet and Sanquer showed that the elastic modulus of linear polyphenyls along the alignment direction of molecules is settled mainly by the force constant for the intra- and inter-molecular bondings of phenyl groups[15]. As the molecular structure of *o*-terphenyl is more complex and bulky, however, the molecular packing and configuration as well as the alignment of phenyl groups may give significant roll on the elastic anisotropy.

The crystal structure of *o*-terphenyl was analyzed from X-ray diffraction by Clews and Lonsdale[5]. The crystallographic data are listed in Table I. The two phenyl groups have their planes turned in the same direction about 45 ~ 50° out of the plane of the parent nucleus. The molecular direction bisecting the angle between the two phenyl bonds lies nearly, but not exactly, along the crystal direction *a*. The molecule, as a whole, is rotated about this direction in such a way that the planes of substituted phenyl groups are more or less normal to *c* axis[5]. As shown in Table I, the axial length of *b* is smaller than the size of the substituted phenyl groups (ca. 0.781 nm), and those groups overlap with those of the neighboring cells. Moreover, the substituted phenyl groups of the second molecule moved through symmetry operator (2_1 axis) at a=1/4 and b=1/2 overlap with those of the first molecule. That is, the substituted phenyl groups are piled up in the direction of c and the contributions of the van-der-Waals' force of the direction of *c* are expected to be stronger than the other directions.

The forces are more efficiently transferred through intra-molecular phenyl bonds. The inclinations of the two phenyl bonds relative to a axis are about 30°, but those to b or c axis are about 67 ~ 71°. As the force constant of stretching is much larger than that of bending and torsion, the efficiency of stretching may be the first to determine the force constant of each direction. Considering the inclinations of the two phenyl bonds, the efficiency of stretching along a axis is 2.3 ~ 2.7 times larger than that along b or c axis, which may give arise to large c_{11} rather than c_{22} or c_{33}. The difference between c_{22} and c_{33} may be due to the difference in their inter-molecular forces (the van-der-Waals' forces) along b and c.

The weak c_{22} of o-terphenyl, which mainly comes from the weak side-to-side van-der-Waals' interaction of phenyl groups, is close to c_{11}, c_{22}, and c_{33} of benzene. The c_{33} of o-terphenyl, which mainly comes from the face-to-face van-der-Waals' interation of phenyl groups, is close to those of c_{11} and c_{22} of biphenyl and p-terphenyl. The small c_{11} of o-terphenyl rather than c_{33} of biphenyl and p-terphenyl may be due to the inclination of the phenyl bond relative to a axis.

The relation of $c_{13} > c_{12} > c_{23}$ of o-terphenyl may approximately reflect the relation of $c_{11} > c_{33} > c_{22}$. The small c_{23} of o-terphenyl compared to c_{12} or c_{13} of biphenyl and p-terphenyl may be caused from that the substituted phenyl groups are nearly normal to c axis and that the deformations such as bending and torsion of the phenyl bonds along b (c) axis cannot effectively be transferred to c (b) axis.

For c_{44}, c_{55}, and c_{66}, we have to consider effects of shear force that brings about rotations of molecules as a whole. The prime factor affecting rotations of molecules is the anisotropy in the inter-molecular interactions of each molecule, which is affected by the anisotropy of the polarizability of each molecule. The value of polarizability tensor of an o-terphenyl molecule can be calculated from that of benzene[16] and hydrogen[17] by assuming additivity and by neglecting volume as

$$\alpha = \begin{pmatrix} 3.18 & 0 & 0 \\ 0 & 3.06 & 3.1 \\ 0 & 3.1 & 22.7 \end{pmatrix} (4\pi\varepsilon_0 \times 10^{-30})\mathrm{m}^3, \tag{34}$$

where the components of the polarizability correspond to the crystallographic coordinates a, b, and c, and ε_0 is the permittivity of vacuum. When the molecule is rotated about a, b, and c axes by infinitesimal angles of $\delta\theta_a$, $\delta\theta_b$, and $\delta\theta_c$, respectively, changes in the polarizability tensor become, to the first order of $\delta\theta_i$, as

$$\Delta\alpha = \left\{ \delta\theta_a \begin{pmatrix} 0 & 0 & 0 \\ 0 & -6.2 & 7.9 \\ 0 & 7.9 & 6.2 \end{pmatrix} + \delta\theta_b \begin{pmatrix} 0 & 3.1 & -9.1 \\ 3.1 & 0 & 0 \\ -9.1 & 0 & 0 \end{pmatrix} + \delta\theta_c \begin{pmatrix} 0 & 1.2 & -3.1 \\ 1.2 & 0 & 0 \\ -3.1 & 0 & 0 \end{pmatrix} \right\} (4\pi\varepsilon_0 \times 10^{-30})\mathrm{m}^3. \tag{35}$$

This equation shows that the change in the polarizability tensor is the smallest in the rotation about c axis. That is, the rotation about c axis rather than about a or b axis is easy, which agrees with the experimental result of $c_{66} < c_{44}, c_{55}$. The small c_{55} rather than c_{44} may be due to packing of the molecule in the crystal cell. The parent phenyl group has some free space along c axis, which may be a cause of the easy rotation about b axis rather than about a axis.

Any pure transverse elastic waves, of which displacements are perpendicular to the scattering plane, have not been observed. In an isotropic media[9], the transverse elastic waves with displacement vectors parallel to the scattering plane do not scatter the light, and those with displacement vectors perpendicular to the scattering plane scatter the light in VH and HV polarizations. The present case is quite inverse to this. In *o*-terphenyl, the molecules align in screw symmetry to three crystal axes. When an *o*-terphenyl molecule rotates by $\delta\theta_i$ about i axis, one neighboring molecule rotates by $-\delta\theta_i$ about the same axis. In the propagation of pure transverse elastic waves bring about only rotations of molecules, therefore, the resultant change in the polarizability tensor becomes zero in the first order of $\delta\theta_i$ as indicated by eq. (35). Since the situation is the same for the dielectric tensor, the scattering of light may be too weak to detect.

As displacement and wave vectors do not meet at right angle in the propagation of pseudo transverse elastic waves, the dilation of the medium takes place together with rotations. Accordingly, the pseudo transverse elastic waves accompany the fluctuation of the polarizability and may scatter the light. Pseudo transverse elastic waves propagating in the plane showing little anisotropy, therefore, would behave similarly to the pure transverse elastic waves and would scatter the light weakly. In the present experiments, the pseudo transverse elastic waves with vector of $\mathbf{K}(0, K_y, K_z)$ could not been observed.

In the Brillouin spectra from two pairs of parallel crystal faces giving the wave vector of $\mathbf{K}(K_x, 0, 0)$ and $\mathbf{K}(0, K_y, 0)$, two Brillouin doublets were observed at 15 and 12 GHz, respectively, as shown in Figure 4. The integrated intensity ratio of the weak doublet to the strong doublet is 0.38 in $\mathbf{K}(K_x, 0, 0)$ and 0.11 in $\mathbf{K}(0, K_y, 0)$. The elastic moduli evaluated from the frequencies of the weak doublets were 20 GPa for $\mathbf{K}(K_x, 0, 0)$ and 5.3 GPa for $\mathbf{K}(0, K_y, 0)$, but their values were found not to fit to the spectra with the another wave vectors at all. Therefore, we have concluded the weak Brillouin doublets to be the stray spectra. The normal incident reflection factor calculated from the index of refraction at a crystal face is at most 7 %, which is fairly small in comparison with the above intensity ratio of the Brillouin doublets. The stray spectra, therefore, may not be brought from scattering of the light internally reflected at crystal faces. The wave and the ray vectors of the light are known to be indeterminate respectively in the directions of the optical (binormals) and the optical ray (biradials) axes[9], which are lying

in the xy plane at the angles of ±60.3° and of ±58.7° to x axis in the o-terphenyl crystal, respectively. The normals of the crystal faces used to observe the Brillouin spectra for the wave vectors of $\mathbf{K}(K_x, 0, 0)$ and $\mathbf{K}(0, K_y, 0)$ lie in the xy plane at the angles of ±57.7° to x axis, which is close to the optical and the optical ray axes. The stray spectra may be caused from this fact.

The attenuation coefficient, $\alpha\lambda_s(= \pi\Delta/v_B)$, roughly increases with decreasing the elastic modulus. The anharmonic term of the potential energy[18,19] and the structural disorder[20–22] also, however, are known to contribute to the attenuation of the elastic waves in solids, which are now being studied.

6. SUMMARY

All of nine elastic constants that represent the elastic term of the free energy of the orthorhombic system of the o-terphenyl single crystal have been determined from the elastic waves observed by the Brillouin light scattering in the following manner: (i) the determination of wave vectors from the dielectric tensor obtained by using a new simple optical method according to the scattering geometry; (ii) the determination of three values of the elastic constants from three pure longitudinal elastic waves by assuming the elastic principal axes to agree with the optical ones; and (iii) the determination of remainder six elastic constants by fitting procedures so as to satisfy the characteristic equation of the wave motion.

The elastic constants of o-terphenyl show intermediate anisotropy between benzene and linear polyphenyls. The anisotropy can reasonably be explained from the arrangement of the phenyl bonds and the inter-molecular interactions caused from the packing of molecules in the crystalline lattice. The polarizability tensor suggests the rotation of the molecule about c axis rather than b or a axis to be easy. In the present crystal system of $P2_12_12_1$, any pure transverse elastic waves will not scatter the light.

References

[1] Y. Higashigaki and C. H. Wang, *J. Chem. Phys*, **74**, 3175 (1981).
[2] G. Fytas, C. H. Wang, D. Lilge, and Th. Dorfmüller, *J. Chem. Phys.*, **75**, 4247 (1981).
[3] C. H. Wang, X. R. Zhu, and J. C. Shen, *Molec. Phys.*, **62**, 749 (1987).
[4] W. Steffen, A. Patkowski, G. Meier, and E. W. Fischer, *J. Chem. Phys.*, **96**, 4171 (1992).
[5] C. J. B. Clews and K. Lonsdale, *Proc. Roy. Soc.*, **A 161**, 493 (1937).
[6] G. Schere, D. R. Uhlmann, C. E. Miller, and K. A. Jackson, *J. Cryst. Growth*, **23**, 323 (1974).
[7] M. Naoki and S. Koeda, *J. Phys. Chem.*, **93**, 948 (1989).
[8] M. Naoki, T. Tanioka, K. Karasawa, and A. Kinoshita, *J. Chem. Phys.*, **94**, 8342 (1991).
[9] L. D. Landau and E. M. Lifshitz, *Electrodynamics of Continuous Media* (Pergamon, Oxford, 1960), 1st ed., Chap. 11, pp. 313–343 and Chap. 14, pp. 377–397.
[10] B. J. Berne and R. Pecora, *Dynamic Light Scattering* (Wiley, New York, 1976), Chap. 3, pp. 24–37.

[11] L. D. Landau and E. M. Lifshitz, *Theory of Elasticity* (Pergamon, London, 1963), 2nd ed., Chap. 1, pp. 1–42 and Chap. 3, pp. 98–118.
[12] M. Born and E. Worf, *Principles of Optics* (Pergamon, Oxford, 1974), 5th ed., Chap. 14.
[13] P. S. Chang and A. B. Bestul, *J. Chem. Phys.*, **56**, 503 (1972).
[14] J. C. W. Heseltine, D. W. Elliott, and O. B. Wilson, Jr., *J. Chem. Phys.*, **40**, 2584 (1964).
[15] C. Ecolivet and M. Sanquer, *J. Chem. Phys.*, **72**, 4145 (1980).
[16] G. R. Alms, A. K. Burnhan, and W. H. Flygare, *J. Chem. Phys.*, **63**, 3321 (1975).
[17] W. Kolos and I. Wolniewicz, *J. Chem. Phys.*, **46**, 1426 (1967).
[18] T. O. Woodruff and H. Ehrenreich, *Phys. Rev.*, **123**, 1553 (1961).
[19] A. A. Maradudin and A. E. Fein, *Phys. Rev.*, **128**, 2589 (1962).
[20] J. D. Eshelby, *Proc. Roy. Soc.*, **A197**, 396 (1949).
[21] F. R. N. Nabarro, *Proc. Roy. Soc.*, **A209**, 278 (1951).
[22] P. G. Kemens, *Proc. Phys. Soc.*, **A168**, 1113 (1955).

Appendix A: Condition for Total Polarization

Let us consider the electromagnetic wave of $n_z = 0$ and $E_z = 0$ incident upon a plane boundary with the outer normal vector of $(e_1, e_2, 0)$. When we take Cartesian coordinates x', y', and z', in which y' axis is along the inner normal of the boundary, $x'z'$ plane is on the boundary plane, and z' axis is antiparallel to z axis, a plane wave expressed by

$$\mathbf{A} = \mathbf{A}_0 e^{-i(\omega t - \mathbf{k}\cdot\mathbf{r})} \tag{A1}$$

satisfies following boundary conditions ($\mathbf{A} = \mathbf{E}, \mathbf{H}$):

$$k_{0x'} = k_{1x'} = K_{2x'}, \tag{A2}$$

$$k_{oz'} = k_{1z'} = K_{2z'}, \tag{A3}$$

$$E_{0x'} = E_{1x'} = E_{2x'}, \tag{A4}$$

$$H_{0z'} = H_{1z'} = H_{2z'}, \tag{A5}$$

where subscripts 0, 1, and 2 denote the incident, reflected, and refracted waves, respectively, and $\mathbf{H}$ is the magnetic field given by

$$\mathbf{H} = [\mathbf{k} \times \mathbf{E}]/\mu_0\omega = (0, 0, k_x E_y - k_y E_x)/\mu_0\omega. \tag{A6}$$

From eqs. (A2) and (A3), we obtain following relations:

$$\theta_0 = \theta_1, \tag{A7}$$

$$\sin\theta_0 / \sin\theta_2 = n_2/n_0 = n, \tag{A8}$$

$$k_{2y'} = \sqrt{k_2^2 - k_{2x'}^2} = k_0\sqrt{n^2 - \sin^2\theta_0}, \tag{A9}$$

where θ_0, θ_1, and θ_2 are the angles of incidence, reflection, and refraction, respectively. Then the vectors $\mathbf{k}_i$, $\mathbf{E}_i$, and $\mathbf{H}_i$ can be expressed by

$$\begin{aligned}
\mathbf{k}_0 &= (k_0 \sin\theta_0, k_0 \cos\theta_0, 0), \\
\mathbf{k}_1 &= (k_o \sin\theta_0, -k_0 \cos\theta_0, 0), \\
\mathbf{k}_2 &= (k_0 \sin\theta_0, k_0\sqrt{n^2 - \sin^2\theta_0}, 0),
\end{aligned} \tag{A10}$$

$$\begin{aligned}
\mathbf{E}_0 &= (E_0 \cos\theta_0, -E_0 \sin\theta_0, 0), \\
\mathbf{E}_1 &= (-E_1 \cos\theta_0, -E_1 \sin\theta_0, 0), \\
\mathbf{E}_2 &= (E_{2x'}, E_{2y'}, 0) = (E_2 \cos\theta_s, -E_2 \sin\theta_s, 0),
\end{aligned} \tag{A11}$$

$$\mathbf{H}_0 = (0, 0, -E_0)\varepsilon_0 c_0,$$
$$\mathbf{H}_1 = (0, 0, -E_1)\varepsilon_0 c_0,$$
$$\mathbf{H}_2 = \left(0, 0, -E_2(\cos\theta_s\sqrt{n^2 - \sin^2\theta_0} + \sin\theta_0 \sin\theta_s)\right)\varepsilon_0 c_0, \quad \text{(A12)}$$

where θ_s is the directional angle of the vector $\mathbf{S}_2$ from y′ axis. Accordingly, eqs. (A4) and (A5) become

$$E_0 \cos\theta_0 - E_1 \cos\theta_0 = E_2 \cos\theta_s, \quad \text{(A13)}$$

$$E_0 + E_1 = E_2(\cos\theta_s\sqrt{n^2 - \sin^2\theta_0} + \sin\theta_0 \sin\theta_s), \quad \text{(A14)}$$

and yield

$$E_1 = E_0 \frac{-\cos\theta_s/\cos\theta_0 + \cos\theta_s\sqrt{n^2 - \sin^2\theta_0} + \sin\theta_0 \sin\theta_s}{\cos\theta_s/\cos\theta_0 + \cos\theta_s\sqrt{n^2 - \sin^2\theta_0} + \sin\theta_0 \sin\theta_s}, \quad \text{(A15)}$$

$$E_2 = E_0 \frac{2}{\cos\theta_s/\cos\theta_0 + \cos\theta_s\sqrt{n^2 - \sin^2\theta_0} + \sin\theta_0 \sin\theta_s}, \quad \text{(A16)}$$

Averaging the real part of the Poynting vector over one cycle, we can obtain the reflected energy flux $\bar{\mathbf{S}}$ as

$$\bar{\mathbf{S}}_1 = E_1^2(\sin\theta_0, -\cos\theta_0, 0)\varepsilon_0 c_0/2. \quad \text{(A17)}$$

Since the electromagnetic wave does not reflect on the boundary,

$$(\bar{S}_{1y'})_{\theta_0=\theta_p} = 0. \quad \text{(A18)}$$

This follows $E_1 = 0$ and the condition for the total polarization is expressed by

$$\cos\theta_s\sqrt{n_p^2 - \sin^2\theta_p} + \sin\theta_p \sin\theta_s = \cos\theta_s/\cos\theta_p, \quad \text{(A19)}$$

$$\frac{\sin\theta_p}{\sin\theta_n} = n_p, \quad (26)$$

or in a reduced form

$$\sin\theta_p \cos\theta_p(1/\tan\theta_n + \tan\theta_s) = 1. \quad \text{(A20)}$$

When α denotes the directional angle of the outer normal vector (e_1, e_2, 0) from x axis, the directional angle of $\mathbf{k}_2$ and $\mathbf{S}_2$ at the total polarization become $(\alpha + \pi - \theta_p)$ and $(\alpha + \pi - \theta_s)$ in the xyz coordinates, respectively, where θ_p and θ_s are defined to take positive sign in the clockwise direction. Then the relation between the directions of $\mathbf{k}$ and $\mathbf{S}$, i.e., eq. (20), is reduced to

$$\tan(\alpha - \theta_s) = \frac{\varepsilon^{(y)}}{\varepsilon^{(x)}}\tan(\alpha - \theta_n). \quad (27)$$